Journal of Mathematical Chemistry 6(1991)281–294

PERMUTATIONAL CHARACTER OF DSD MECHANISMS IN HEPTACOORDINATE CHEMISTRY

J. BROCAS and M. BAUWIN

Chimie Organique Physique, Faculté des Sciences, Université Libre de Bruxelles, 50, Avenue F.D. Roosevelt, B-1050 Bruxelles, Belgium

Received 1 June 1990
(Revised 13 September 1990)

Abstract

The permutational character of degenerate single and double dsd and of degenerate 4, 5-pyramidal processes is obtained for the heptacoordinate deltahedra. The symmetry properties of the paths of steepest descent and transition states of these rearrangements are derived. From this permutational character, it would be possible to investigate the compatibility of these processes with the results of NMR line shape analysis of the dynamics of heptacoordinate complexes. This possibility is briefly discussed.

1. Introduction

Permutational analysis of the static and dynamic stereochemistry of ML_n complexes (M = central atom, L = ligand) has been used extensively in recent years. In this method, the $n!$ permutations of the ligands on the sites of the molecular skeleton give rise to

$$p = \frac{n!}{|A|} \tag{1}$$

configurations. Interconversions of these configurations are described by modes of rearrangements. The number of such modes is

$$z = \frac{n!}{|A||G|} \sum_y \left\{ \frac{|A \cap C_y|^2}{|C_y|} + \frac{|A\sigma \cap C_y|^2}{|C_y|} \right\}. \tag{2}$$

Details about these concepts may be found in, for instance, refs. [1–3]. In the above formula, A and G denote the group of proper symmetry operations of the molecular skeleton and its point group:

$$G = A \cup A\sigma,$$

where σ is any improper operation, C_y are the classes of S_n, the symmetric group of degree n, and $|A|$ is the order of A. The symbols $\cup$ and $\cap$ refer to union and intersection, respectively.

The number of configurations and the number of modes increase rapidly when n jumps from 5 or 6 to 7. For instance, if we calculate them for trigonal bipyramidal ($n = 5$), octahedral ($n = 6$) and pentagonal bipyramidal ($n = 7$) geometries, we find, respectively, $p = 20$, 30 and 504 and $z = 6$, 5 and 40. For this reason, a systematic and exhaustive permutational analysis of the dynamic stereochemistry of ML_7 complexes seems impracticable.

A different and interesting point of view has been developed by King [4,5]: the ML_n complexes are described as n-vertex polyhedra. The polyhedra having only triangular faces are supposed to be energetically favoured. These so-called deltahedra interconvert through dsd processes, which involve removal and subsequent addition of an edge (see fig. 1).

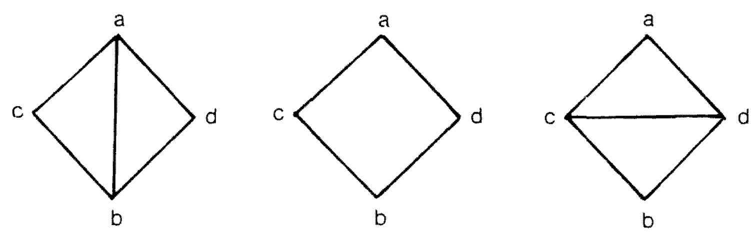

Fig. 1. The single dsd process.

Such processes are also energetically favoured since only two triangular faces are lost and replaced by a quadrilateral face in the intermediate state. King's assumptions described above are based on a previous structural and mechanistic study of boranes and carboranes [6].

King has established the list of single and double degenerate dsd for heptacoordinate deltahedra [5]. In such degenerate dsd, the starting and final deltahedra are identical, up to a permutation or a permutation–inversion of the vertices, i.e. they correspond to a permutational mode of rearrangements [3].

In the present paper, we determine the permutational character [3] of the degenerate single and double dsd listed by King. As we will see, some of these double dsd can only give rise to a final configuration which is identical to the starting one. Such processes do not give rise to ligand scrambling (they are described by the identity permutation). The remaining processes are the only interesting ones in view of their comparison with the NMR line shape analysis on heptacoordinate deltahedra.

2. The dsd mechanisms

We first recall the list of 34 polyhedra with seven vertices. This has been obtained by Britton and Dunitz [7], and derived independently by King [5] from the 34 polyhedra with seven faces [8]. The 34 polyhedra having seven vertices are displayed in table 1. The columns BD and K refer to the numbers used by

Table 1

The 34 polyhedra

	v_i				f_j				e_{kl}											
BD	6	5	4	3	6	5	4	3	33	34	35	36	44	45	46	55	56	66	K	SYM
1	1	3	0	3	0	0	0	10	0	0	6	3	0	0	0	3	3	0	#12	C_{3v}
2	2	0	3	2	0	0	0	10	0	2	0	4	2	0	6	0	0	1	#11	C_{2v}
3	1	2	2	2	0	0	0	10	0	2	2	2	0	4	2	1	2	0	#13	C_2
4	0	3	3	1	0	0	0	10	0	0	3	0	3	6	0	3	0	0	#20	C_{3v}
5	0	2	5	0	0	0	0	10	0	0	0	0	5	10	0	0	0	0	#23	D_{5h}
6	1	1	2	3	0	0	1	8	0	4	2	3	0	2	2	0	1	0	#14	C_s
7	1	1	2	3	0	0	1	8	1	2	2	3	1	2	2	0	1	0	#15	C_1
8	0	3	1	3	0	0	1	8	1	1	6	0	0	3	0	3	0	0	#21	C_s
9	0	3	1	3	0	0	1	8	0	2	7	0	0	2	0	3	0	0	#22	C_s
10	1	0	4	2	0	0	1	8	0	4	0	2	4	0	4	0	0	0	#16	C_{2v}
11	0	2	3	2	0	0	1	8	0	2	4	0	2	6	0	0	0	0	#24	C_s
12	0	2	3	2	0	0	1	8	0	3	3	0	2	5	0	1	0	0	#25	C_1
13	0	1	5	1	0	0	1	8	0	2	1	0	7	4	0	0	0	0	#28	C_s
14	1	0	2	4	0	1	0	7	2	4	0	4	1	0	2	0	0	0	#17	C_s
15	0	1	3	3	0	1	0	7	1	5	2	0	2	3	0	0	0	0	#29	C_s
16	1	0	2	4	0	0	2	6	2	4	0	4	1	0	2	0	0	0	#18	C_{2v}
17	0	2	1	4	0	0	2	6	2	2	6	0	0	2	0	1	0	0	#26	C_1
18	0	2	1	4	0	0	2	6	2	2	6	0	0	2	0	1	0	0	#27	C_2
19	0	1	3	3	0	0	2	6	1	4	3	0	3	2	0	0	0	0	#33	C_1
20	0	1	3	3	0	0	2	6	1	5	2	0	2	3	0	0	0	0	#32	C_1
21	0	1	3	3	0	0	2	6	0	7	2	0	1	3	0	0	0	0	#30	C_s
22	0	1	3	3	0	0	2	6	0	6	3	0	2	2	0	0	0	0	#31	C_s
23	0	0	5	2	0	0	2	6	1	4	0	0	8	0	0	0	0	0	#36	C_{2v}
24	0	0	5	2	0	0	2	6	0	6	0	0	7	0	0	0	0	0	#37	C_2
25	1	0	0	6	1	0	0	6	6	0	0	6	0	0	0	0	0	0	#19	C_{6v}
26	0	1	1	5	0	1	1	5	4	3	4	0	0	1	0	0	0	0	#34	C_1
27	0	0	3	4	0	1	1	5	3	6	0	0	3	0	0	0	0	0	#38	C_s
28	0	1	1	5	0	0	3	4	4	3	4	0	0	1	0	0	0	0	#35	C_s
29	0	0	3	4	0	0	3	4	3	6	0	0	3	0	0	0	0	0	#40	C_{3v}
30	0	0	3	4	0	0	3	4	2	8	0	0	2	0	0	0	0	0	#42	C_1
31	0	0	3	4	0	0	3	4	2	8	0	0	2	0	0	0	0	0	#41	C_2
32	0	0	3	4	0	0	3	4	3	6	0	0	3	0	0	0	0	0	#39	C_{3v}
33	0	0	1	6	0	1	2	3	7	4	0	0	0	0	0	0	0	0	#43	C_s
34	0	0	1	6	0	0	4	2	7	4	0	0	0	0	0	0	0	0	#44	C_{2v}

Britton–Dunitz and King, respectively. In the present paper, we will denote polyhedron 12 in King's numbering by #12. The last column gives the maximum possible symmetry of each polyhedron, i.e. the symmetry of the graph representing the polyhedron. The symbols v_i, f_j and e_{kl} are, respectively, the number of vertices of degree i, the number of faces having j edges, and the number of edges connecting vertices of degree k and l. Note that these three sets of numbers are the same for #26 and #27. These polyhedra differ by the symmetry of their graphs and by the fact that their two edges connecting vertices of degree three are connected in #26 and disconnected in #27.

Now let us focus on #11, #12, #13, #20, #23, which are deltahedra, i.e. they have only triangular faces. Let v, e, f be the number of vertices, edges and faces, respectively. The Euler relation $e + 2 = f + v$, valid for convex polyhedra, and the relation $2e = 3f$, valid for deltahedra, impose $f = 10$ and $e = 15$ for heptacoordinate deltahedra. The five deltahedra are represented in fig. 2, where the vertices have been numbered for further use.

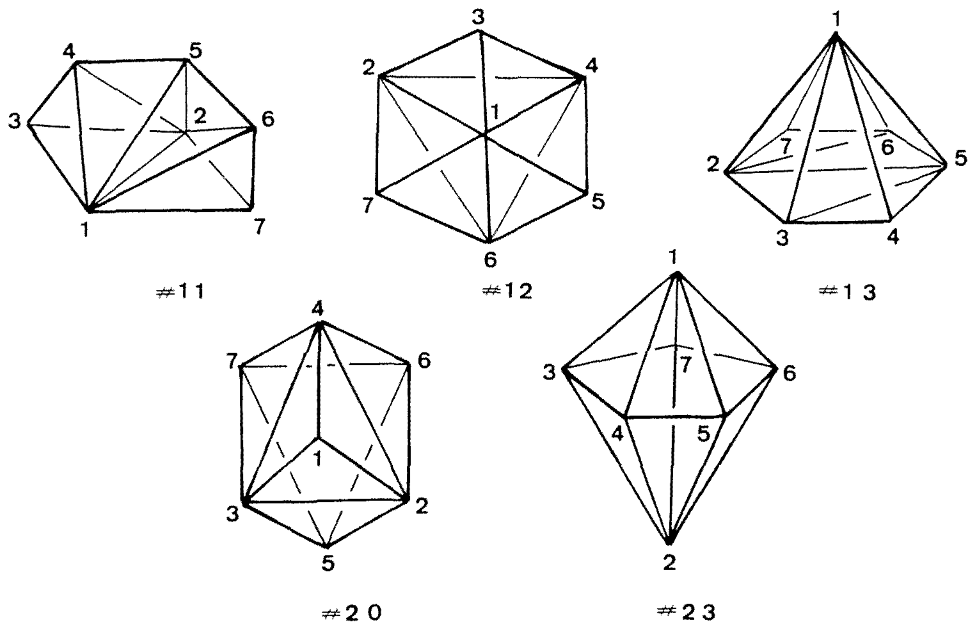

Fig. 2. The five deltahedra.

From each of these deltahedra, we now remove two edges. After removal of the first one, the resulting polyhedron has 1 quadrilateral and 8 triangular faces (#14, #15, #16, #21, #22, #24, #25, #28). After removal of the second edge, it possesses either 2 quadrilateral faces and 6 triangular ones (#18, #26, #27, #30, #31, #32, #33, #36, #37) or 1 pentagonal and 7 triangular faces (#17, #29). These double edge removals are best represented [9] by a directed graph whose vertices are the polyhedra and whose directed edges (arrows) represent polyhedron edge removal (see fig. 3). This graph is easy to obtain from table 1 in ref. [5] or from table 1 in ref. [7]. Note that in fig. 3, the vertices with an asterisk denote a pair of enantiomeric polyhedra.

We notice that 1 or 2 arrows end at the polyhedra having 1 quadrilateral face and 8 triangular faces (type II in fig. 3). Indeed, the quadrilateral face can be diagonalised

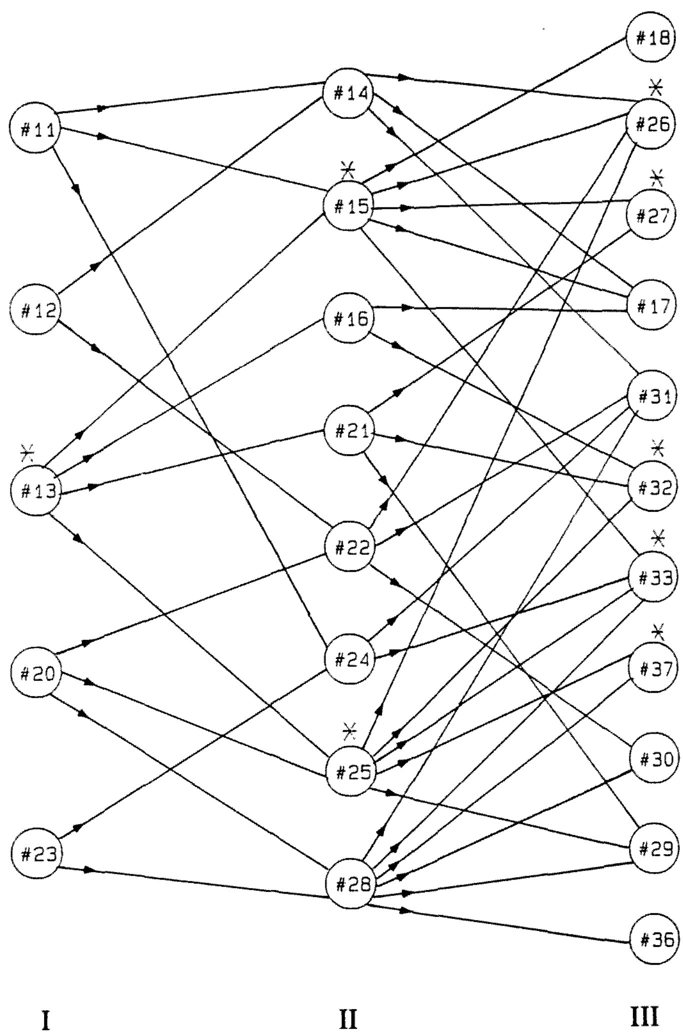

Fig. 3. Polyhedron edge removals.

in two ways, leading back to 2 deltahedra which can be either distinct or identical, up to a permutation or a permutation–inversion of the vertices. In the second case, the transformation leading from one of the deltahedra to the other with an intermediate of type II is clearly a degenerate single dsd. From fig. 3, it appears that there are two such possibilities:

$$\#13 \to \#16 \to \#13$$
$$\#13 \to \#21 \to \#13. \tag{3}$$

A similar argument may be used to find degenerate processes leading from one deltahedron to another with an intermediate of type III. If this intermediate has two quadrilateral faces, the process is a degenerate double dsd. If it has a pentagonal face, the process is a so-called degenerate 4-pyramidal combined with a 5-pyramidal process [5] (in short, 4, 5-pyramidal process).

Complete diagonalisation of a polyhedron of type III and having two quadrilateral faces may be realised in eight ways. Indeed, the first diagonal can be added in four ways and the second quadrilateral face can be diagonalised in two ways. If two ways differ only by the order in which two given diagonals are added, they lead to the same deltahedron. Hence, the paths leading to a given polyhedron of type III and having two quadrilateral faces start from at most four deltahedra. In a similar way, one shows that the number of starting deltahedra leading to a polyhedron of type III with one pentagonal face is at most five. These starting deltahedra are listed in table 2 for

Table 2

Starting polyhedra (noted +) for each polyhedron of type III

Polyhedron of type III	Starting deltahedron				
	#11	#12	#13	#20	#23
#18	+		+		
#26	+	+	+	+	
#27	+		+		
#30		+		+	+
#31	+	+		+	+
#32			+	+	
#33	+		+	+	+
#36				+	+
#37			+	+	+
#17	+	+	+		
#29			+	+	+

each polyhedron of type III. If the number of starting deltahedra is less than four (five, if a pentagonal face is involved), there exists a possibility of degenerate double dsd (or of a 4, 5-pyramidal degenerate process). Such possibilities do not exist with #26, #31 and #33 as intermediates, as shown by table 2.

From table 2, the remaining possibilities are listed below:

#11 → #18 → #11 †
#13 → #18 → #13 †

#11 → #27 → #11
#13 → #27 → #13 †

$$
\begin{array}{l}
\#12 \rightarrow \#30 \rightarrow \#12 \\
\#20 \rightarrow \#30 \rightarrow \#20\ \dagger \\
\#23 \rightarrow \#30 \rightarrow \#23 \\[6pt]
\#13 \rightarrow \#32 \rightarrow \#13\ \dagger \\
\#20 \rightarrow \#32 \rightarrow \#20 \\[6pt]
\#20 \rightarrow \#36 \rightarrow \#20\ \dagger \\
\#23 \rightarrow \#36 \rightarrow \#23\ \dagger \\[6pt]
\#13 \rightarrow \#37 \rightarrow \#13 \\
\#20 \rightarrow \#37 \rightarrow \#20\ \dagger \\
\#23 \rightarrow \#37 \rightarrow \#23 \\[6pt]
\#11 \rightarrow \#17 \rightarrow \#11\ \dagger \\
\#12 \rightarrow \#17 \rightarrow \#12 \\
\#13 \rightarrow \#17 \rightarrow \#13 \\[6pt]
\#13 \rightarrow \#29 \rightarrow \#13 \\
\#20 \rightarrow \#29 \rightarrow \#20\ \dagger \\
\#23 \rightarrow \#29 \rightarrow \#23
\end{array}
\tag{4}
$$

3. Permutational character of dsd mechanisms

In this section, we establish the permutational character of the possible dsd mechanism listed in eqs. (3) and (4).

The degenerate single dsd starting from deltahedra and listed in eq. (3) are represented in fig. 4. The maximum symmetry of each polyhedron is indicated (see table 1). The crosses indicate the edges of the starting (left) or final (right) deltahedra that do not appear in the intermediate state (center) (polyhedron of type II in the present case). A process such as #13 → #16 → #13 is denoted by #13/16.

The degenerate double dsd or the 4, 5-pyramidal degenerate processes may be found by inspecting the possibilities shown in eq. (4). It appears that each intermediate of type III in this equation gives rise to at least one degenerate process, denoted by a dagger in eq. (4). Processes without a dagger may in fact only be realised in a trivial way (i.e. by first suppressing two edges and subsequently adding the two edges which have first been suppressed). For instance, in fig. 5 two edges (denoted by a cross) have been suppressed on the starting polyhedron #12, giving rise to #30 (fig. 5(a)). A deltahedron may be obtained by diagonalising the two square faces of #30. This may be realised by adding to #30 one of the following pairs of edges: {14, 16}, {14, 57}, {35, 16}, {35, 57}. The first of these four possibilities generates a final configuration of #12 which is identical to the initial one, since no edges have been switched. This process #12 → #30 → #12 may be represented by the identity permutation. The second and third possibilities are in fact single dsd's, since only one diagonal

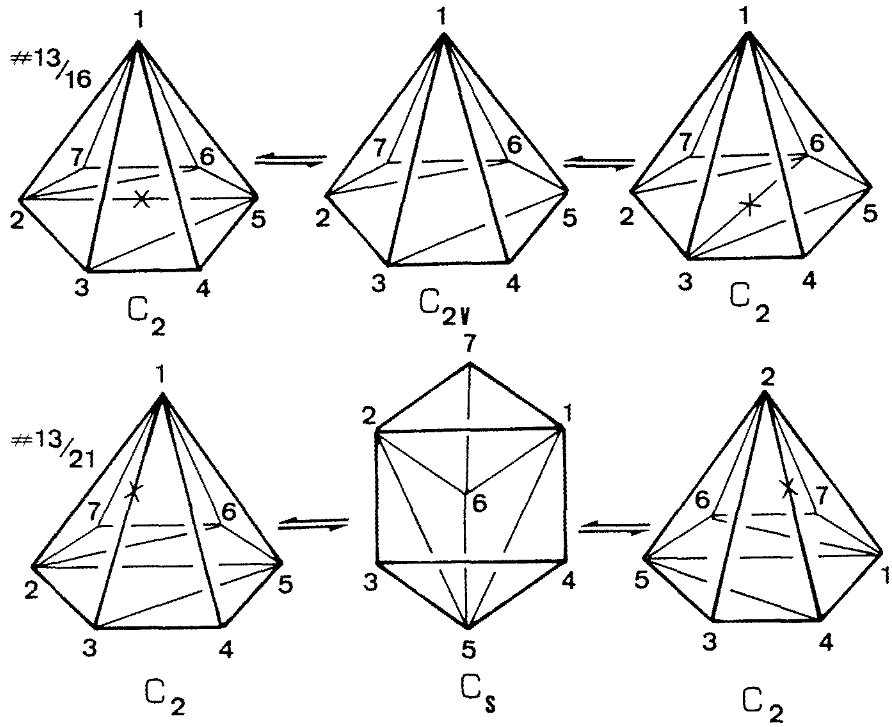

Fig. 4. Degenerate single dsd of deltahedron #13.

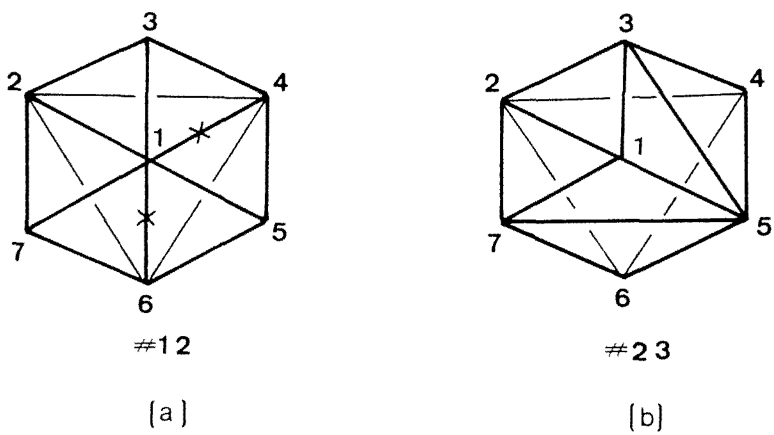

Fig. 5. Non-degenerate double dsd of deltahedron #12.

has been switched. The last possibility gives rise to a deltahedron with no vertex of degree 6 (fig. 5(b)). Hence, it cannot be #12. In fact, the overall course of this last possibility is the double *non*-degenerate dsd #12 → #22 → #30 → #28 → #23 (see fig. 3). Hence, the process #12 → #30 → #12 may only be realised in a trivial way.

Degenerate processes with polyhedra of type III as intermediate are listed in figs. 6 to 9. The symbols are the same as in fig. 4. Moreover, a process such as #11 $\rightarrow$ #14, #15 $\rightarrow$ #17 $\rightarrow$ #14, #15 $\rightarrow$ #11, where #14 and #15 are the only polyhedra of type II that can be traversed (see fig. 3) will henceforth be denoted by #11/17.

From figs. 4 and 6 to 9, it is easy to deduce the permutations or permutations–inversions transforming the starting deltahedron (left) into the final one (right). The results are shown in table 3. The presence of J (inversion about the center of mass) results from the fact that the starting and final skeleta are enantiomeric. The permutations have the same meaning as in ref. [10].

Table 3

Permutations or permutation–inversions for the single and double dsd and the 4, 5-pyramidal processes of the deltahedra

Type		Permutation (Inversion)
#11/18	double dsd	(152) (34) (67)
#11/17	4, 5-pyramidal	(146) (357)
#13/16	single dsd	(16) (35) . J
#13/21	single dsd	(12) (34) . J
#13/18	double dsd	(25) (34) (67) . J
#13/27	double dsd	(152) (34) (67)
#13/32	double dsd	(12473) (56)
#20/30	double dsd	(16327)
#20/37	double dsd	(15) (27) (46)
#20/36	double dsd	(13) (27) (45)
#20/29	4, 5-pyramidal	(123) (45) (67)
#23/36	double dsd	(1623)

From the permutations describing the various degenerate processes listed in table 3, it is easy to verify that these processes belong to different modes of rearrangements of the deltahedra from which they start. Moreover, it is possible to determine the symmetry of the path of steepest descent and transition state (PSD/TS) [10] of these rearrangements [11]. The results are given in table 4, where $\tilde{A}$, $\tilde{R}$ are the group of proper symmetry operations and the point group of the PSD, respectively, whereas A_T, R_T denote similar groups for the TS. The connectivity δ is also given and represents the number of configurations reached in one step of the considered rearrangement, starting from a fixed arbitrary configuration [11, 12]. All these rearrangements are self-inverse (SI) [13] except for #13/32, which is a non-self-inverse (NSI) rearrangement. This may be verified in figs. 4 and 6 to 9 by noting, for instance, that "crossed" edges of the starting deltahedra are equivalent to those of the final one in all rearrangements but #13/32. This indeed means that the direct and reverse rearrangements #13/32 are themselves mutually inverse non-equivalent stereochemical courses.

Table 4

PSD and TS symmetry

Rearrange-ment	δ	$\tilde{A}$	$\tilde{R}$	A_T	R_T	
#11/18	2	I	$\tilde{A} \cup (37)(46)J$	$\tilde{A} \cup (15)(36)(47)$	$A_T \cup \{(15)(34)(67),(37)(46)\}J$	C_{2v}
#11/17	4	I	$\tilde{A}$	$\tilde{A}$	$\tilde{A} \cup (16)(35)J$	C_s
#13/16	2	I, (25)(36)(47)	$\tilde{A}$	$\tilde{A}$	$\tilde{A} \cup \{(23)(47)(56),(26)(35)\}J$	C_{2v}
#13/21	4	I	$\tilde{A}$	$\tilde{A}$	$\tilde{A} \cup (12)(34)J$	C_s
#13/18	2	I, (25)(36)(47)	$\tilde{A}$	$\tilde{A}$	$\tilde{A} \cup \{(37)(46),(25)(34)(67)\}J$	C_{2v}
#13/27	2	I	$\tilde{A}$	$\tilde{A} \cup (12)(37)(46)$	A_T	C_2
#13/32	2	I	$\tilde{A}$	I	A_T	C_1
#20/30	6	I	$\tilde{A}$	$\tilde{A}$	$\tilde{A} \cup (17)(26)J$	C_s
#20/29	6	I	$\tilde{A}$	$\tilde{A}$	$\tilde{A} \cup (13)(45)J$	C_s
#20/37	6	I	$\tilde{A}$	$\tilde{A} \cup (15)(27)(46)$	A_T	C_2
#20/36	3	I	$\tilde{A} \cup (24)(57)J$	$\tilde{A} \cup (13)(27)(45)$	$A_T \cup \{(13)(25)(47),(24)(57)\}J$	C_{2v}
#23/36	10	I, (12)(36)(45)	$\tilde{A}$	$\tilde{A}$	$\tilde{A} \cup \{(13)(26)(45),(16)(23)\}J$	C_{2v}

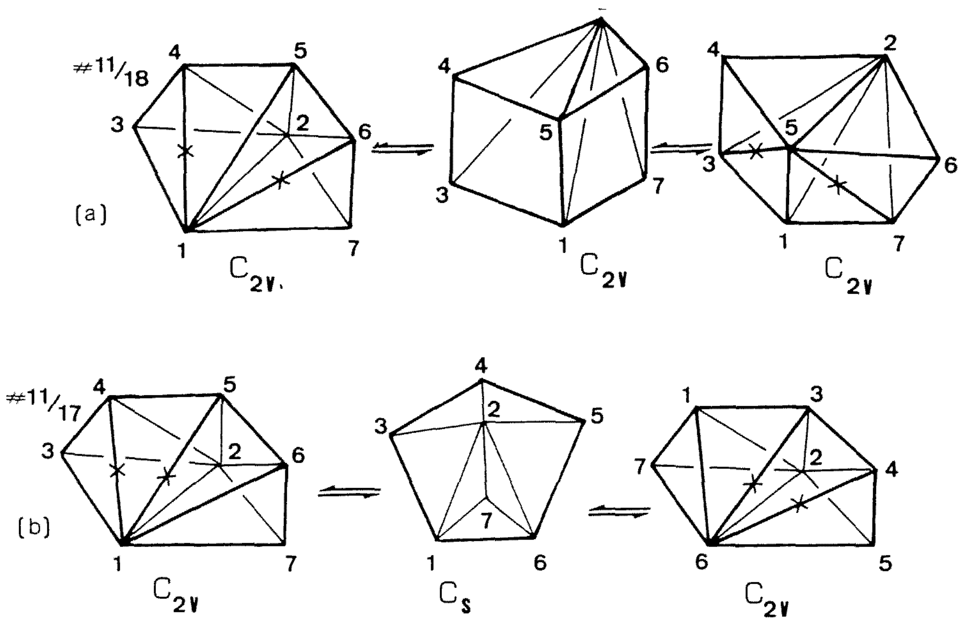

Fig. 6. (a) Degenerate double dsd, and (b) degenerate 4, 5-pyramidal process of deltahedron #11.

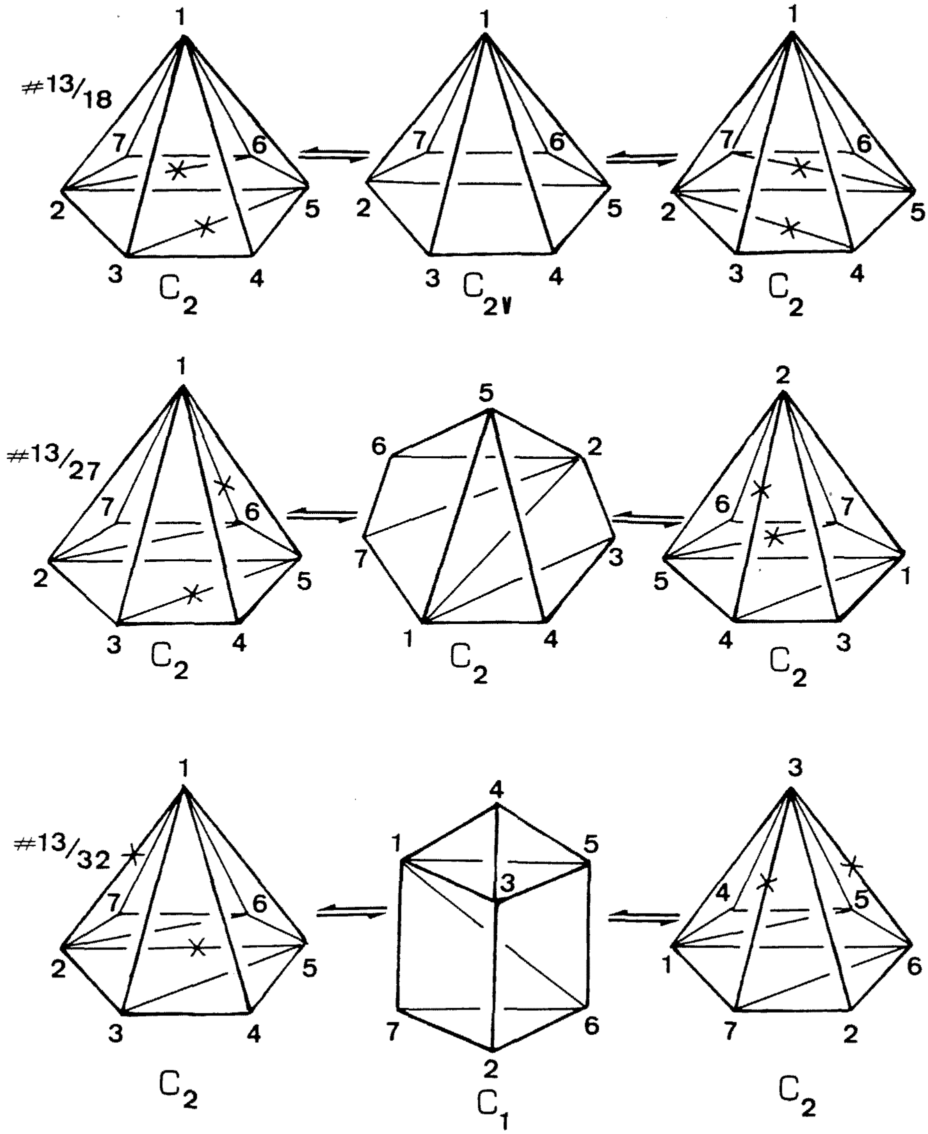

Fig. 7. Degenerate double dsd of deltahedron #13.

The last column in table 4 refers to the point groups of the TS of each rearrangement, i.e the maximum symmetry compatible with a simple saddle point TS connected to reactant and products by PSDs. In the present case, these TS symmetries coincide with the graph symmetries listed in table 1. For instance, the double dsd #11/18 has a C_{2v}–TS symmetry (table 4) and the intermediate polyhedron of type III, i.e. #18, has also a C_{2v}–graph symmetry (table 1). It should, however, be noted that this coincidence is *not* a general rule. A counterexample has recently been discussed [14]:

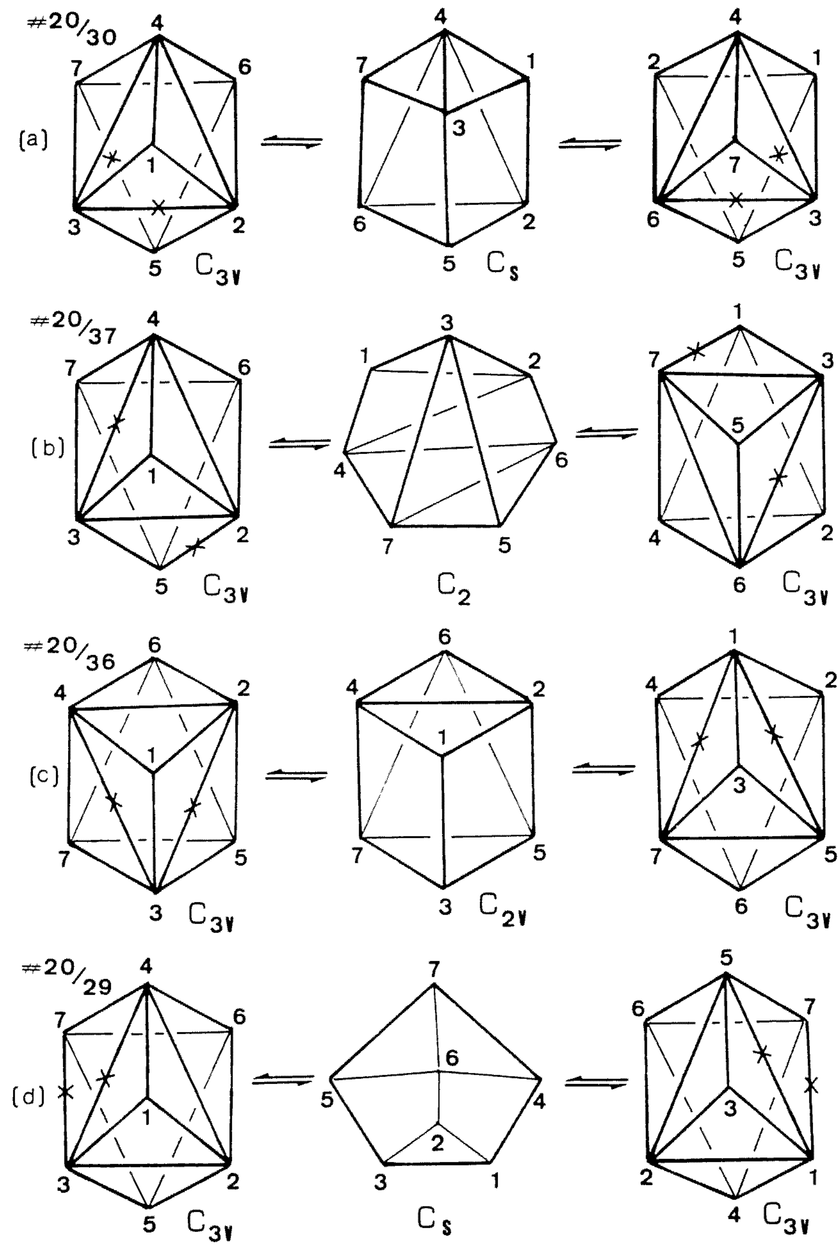

Fig. 8. (a,b,c) Degenerate double dsd, and (d) degenerate 4, 5-pyramidal process of deltahedron #20.

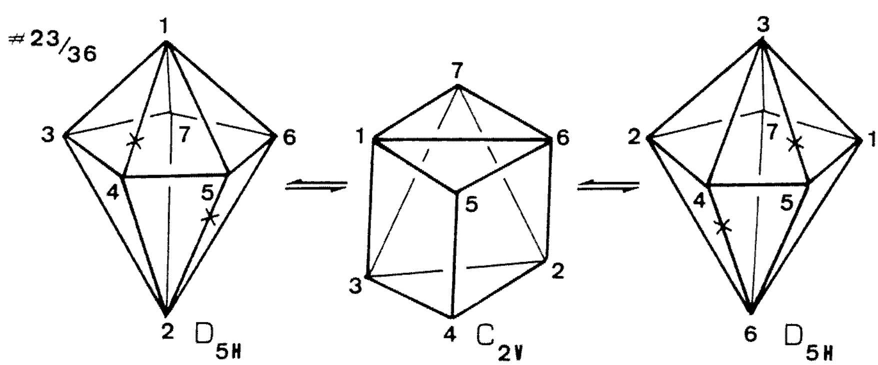

Fig. 9. Degenerate double dsd of deltahedron #23.

if octacoordinate square antiprisms are assumed to undergo a $\pi/4$ rotation of their square faces, they traverse an intermediate whose TS-symmetry is D_{4h} but whose graph symmetry is O_h.

4. Conclusions

In this paper, we have established the complete list of degenerate single and double dsd and of degenerate 4, 5-pyramidal processes for heptacoordinate deltahedra. We have determined the permutational character of these processes. The symmetry properties of the paths of steepest descent and transition states of such stereochemical events have also been obtained.

Theoretical considerations [15] have shown that the most stable deltahedra are the capped octahedron (#20) and the pentagonal bipyramid (#23). The non-deltahedral 4-capped trigonal prism (#36) is of comparable stability.

These three polyhedra, as well as the so-called 4:3 piano stool, have been studied experimentally. The permutational character of the rearrangements of various complexes displaying such geometries has been obtained (or can be obtained) from NMR line shape analysis (see, e.g. [16–20] and references cited therein).

It seems interesting to compare the theoretical permutational character of the processes studied in the present work to the results of the current experimental work, in order to decide whether the observed behaviour is compatible with degenerate dsd or 4, 5-pyramidal processes.

On the other hand, the interconversions of heptacoordinate molecules have also been described in terms of the two following pathways [21,22]:

(a) pentagonal bipyramid (#23) → capped octahedron (#20) → 4-capped trigonal prism (#36) with retention of a mirror plane;

(b) 4-capped trigonal prism (#36) → pentagonal bipyramid (#23) with retention of a twofold axis.

The latter possibility (b) is clearly related to the degenerate double dsd shown in fig. 9. The former (a) could provide interesting alternatives to degenerate dsd or 4, 5-pyramidal processes and should also be compared to the results of NMR line shape analysis.

These tasks will be undertaken in the near future.

Acknowledgement

We thank Mr. R. Vandeloise for computer-assisted drawing of some graphs.

References

[1] W. Hässelbarth and E. Ruch, Theor. Chim. Acta 29(1973)259.
[2] W.G. Klemperer, J. Amer. Chem. Soc. 94(1972)8360.
[3] J. Brocas, M. Gielen and R. Willem, *The Permutational Approach to Dynamic Stereochemistry* (McGraw–Hill, New York, 1983).
[4] R.B. King, Inorg. Chim. Acta 49(1981)237.
[5] R.B. King, Inorg. Chem. 24(1985)1716.
[6] W.N. Lipscomb, Science (Washington, DC) 153(1966)373.
[7] D. Britton and J.D. Dunitz, Acta Cryst. 29A(1973)362.
[8] P.J. Federico, Geometriae Dedicata 3(1975)469.
[9] M. Bauwin, Mémoire de Licence (Université Libre de Bruxelles, 1989).
[10] P. Pechukas, J. Chem. Phys. 64(1976)1516.
[11] J. Brocas and R. Willem, J. Amer. Chem. Soc. 105(1983)2217.
[12] E.L. Muetterties, J. Amer. Chem. Soc. 91(1969)1636; 4115.
[13] J.G. Nourse, J. Amer. Chem. Soc. 102(1980)4883;
D.J. Klein and A.H. Cowley, J. Amer. Chem. Soc. 97(1975)1633.
[14] J. Brocas, in: *Advances in Dynamic Stereochemistry*, ed. M. Gielen (Freund Publ., 1985), p. 43.
[15] D.L. Kepert, *Inorganic Stereochemistry* (Springer, New York, 1982).
[16] S.J. Lippard, Progr. Inorg. Chem. 21(1976)91.
[17] S. Datta, B. Dezube, J.K. Kouba and S.S. Wreford, J. Amer. Chem. Soc. 100(1978)4404.
[18] J.L. Templeton and B.C. Ward, Inorg. Chem. 19(1980)1753; J. Amer. Chem. Soc. 103(1981)3743.
[19] F.A. Van-Catledge, S.D. Ittel and J.P. Jesson, Organometallics 4(1985)18.
[20] P.K. Baker and S.G. Fraser, Polyhedron 12(1987)2081.
[21] E.L. Muetterties, Tetrahedron 30(1974)1595.
[22] B.W. Clare, M.C. Favas, D.L. Kepert and A.S. May, in: *Advances in Dynamic Stereochemistry*, ed. M. Gielen (Freund Publ., 1985), p. 1.